Simulated annealing study of gyroid formation in diblock copolymer solutions

Pingchuan Sun,[1] Yuhua Yin,[2] Baohui Li,[2,*] Tiehong Chen,[1] Qinghua Jin,[2] Datong Ding,[2] and An-Chang Shi[2,3]
[1]*Key Laboratory of Functional Polymer Materials, Ministry of Education, College of Chemistry, Nankai University, Tianjin 300071, China*
[2]*College of Physics, Nankai University, Tianjin 300071, China*
[3]*Department of Physics and Astronomy, McMaster University, Hamilton, Ontario L8S 4M1, Canada*
(Received 31 May 2005; published 30 December 2005)

Conditions for the formation of gyroid structures in diblock copolymer solutions are examined using a simulated annealing technique. The simulations were performed on diblock copolymer systems of $A(N_A)$-b-$B(N_B)$ (with $N_A < N_B$) in solvents that are selective to the A blocks. It is shown that gyroid structures form in a narrow range of block copolymer concentrations between the hexagonally packed cylindrical and the lamellar phases and at an almost constant B-monomer concentration. It is also shown that the gyroid structure is especially sensitive to the B-solvent interaction (ε_{BS}) and the length of the B block (N_B). Phase diagrams for the diblock copolymer solutions are constructed. These predicted results are consistent with previous experimental observations. The three-dimensional isosurface contour plots of the simulated gyroid structure shows two interpenetrating strut networks. The projection along the [111] direction of the simulated gyroid structure and the spherically averaged structure factor are in good agreement with previous experimental results.

DOI: 10.1103/PhysRevE.72.061408 PACS number(s): 82.70.−y, 81.16.Dn

INTRODUCTION

Due to their ability to self-assemble into various ordered microstructures, block copolymers have been studied for many years with tremendous scientific interests [1,2]. Several comprehensive reviews on both theoretical and experimental studies of block copolymer phase behavior are available [3–6]. Of the morphologies commonly observed in diblock copolymers, the gyroid structure is the most intriguing. Gyroid is a bicontinuous cubic structure with $Ia\bar{3}d$ symmetry. Typically, gyroid structures exist in a narrow region between the hexagonally packed cylindrical and the lamellar phases [7,8]. For diblock copolymers with appropriate composition in melt, the shorter segment forms interweaving left- and right-handed threefold coordinated strut networks [9–14]. A good review of the equilibrium phase behavior of diblock copolymers is given by Matsen [15]. Order-order phase transitions (OOTs) between morphologies of different symmetry, involving the gyroid have been investigated both experimentally [16–22] and theoretically [23–25] in diblock copolymer melts.

The addition of homopolymers or solvents to block copolymers provides extra degrees of freedom to control morphologies and hence structure-property relationships [26–33]. For diblock copolymers in selective solvents, formation of gyroid structures has been observed experimentally at different concentrations, and the phase behavior depends on the copolymer composition and the solvent selectivity [34–37]. Quite recently, kinetics of OOTs involving the gyroid has been investigated in diblock copolymer solutions [38–40]. These experimental works and computer simulations [41] have suggested that block copolymer solutions possess some advantages over melts in terms of studying OOTs. The use of solvents of differing selectivity and the temperature dependence of the selectivity can provide access to several different OOTs for a single block copolymer.

In order to understand and control the OOTs involving the gyroid, it is important to obtain the conditions for the formation of the gyroid structure. However, it has been shown that locating the gyroid is a difficult task due to the complexity of the structure [42–48]. In this paper, we study the condition of the formation of gyroid structures in diblock copolymer solutions. The system is composed of $A(N_A)$-b-$B(N_B)$ diblock copolymers (with $N_A < N_B$) in selective solvents for the A segment and equilibrium morphologies of the system are obtained using the simulated annealing method. The simulated annealing technique is a well-known procedure [49] for obtaining the lowest-energy "ground states" in disordered systems [50]. Larson [51] has applied the annealing idea in his studies of the self-assembly of surfactants and block copolymers in an oil-water system. Chakrabarti *et al.* [52] have applied the simulated annealing method to avoid the formation of defect in the lamellar formed through the self-assembling of block copolymers. In our previous studies, we have demonstrated that the simulated annealing is an efficient method for studying the self-assembly morphologies of block copolymers in solutions [41,53,54] or in confined environments [55]. In the work reported here, we performed simulations to seek the conditions for the formation of gyroid structures in $A(N_A)$-b-$B(N_B)$ diblock copolymers (with $N_A < N_B$) in selective solvents. A series of copolymer compositions is examined, in which the longer segments (B) form the network structure whereas the shorter segments (A), together with solvents, form the matrix. In a related paper published elsewhere [41], we investigated the morphological transitions involving gyroid structures in an asymmetric diblock copolymer [$A(3)$-b-$B(9)$] in A-selective solvents, in which

*Author to whom correspondence should be addressed. Fax: +86-22-23501490. Email address: baohui@nankai.edu.cn

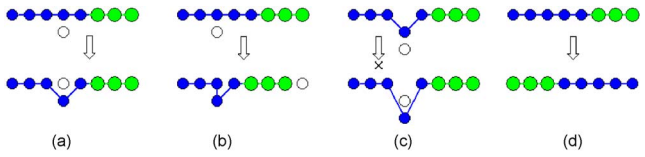

FIG. 1. (Color online) Schematic depiction of the trial moves used in the simulated annealing. Solid circles represent monomers on the chain; open circles represent solvent molecules.

the shorter segment (A) forms the gyroid structure and that the copolymer concentrations are relatively high.

MODEL AND SIMULATION METHOD

The Monte Carlo simulation studies were carried out using a simulated annealing method. The "single-site bond fluctuation" model proposed by Carmesin and Kramer [56] and by Larson [51] was used to implement the Monte Carlo technique. For completeness, the model and algorithm are briefly reviewed in this section. The binary systems under investigation are composed of two components, i.e., diblock copolymers $A(N_A)$-b-$B(N_B)$ and solvents. The numbers of diblock copolymer chains and solvent molecules are denoted as N_C and N_S, respectively. Each diblock copolymer is a chain composed of N_A A monomers and N_B B monomers. Each copolymer chain has $N=N_A+N_B$ monomers in total. A series of N_A and N_B are studied. The system is embedded in a simple cubic lattice of volume $V=L\times L\times L$. The total monomer concentration and the B monomer concentration are defined as $c_p=N_cN/V$ and $c_B=N_cN_B/V$, respectively. Periodic boundary conditions are used in all three directions. Each monomer occupies one lattice site and the copolymers are self- and mutually avoiding, i.e., no two monomers can occupy any one site simultaneously. The bond length is equal to 1 and $\sqrt{2}$, i.e., each site has 18 nearest neighbor sites.

For the problem of interest in the current study, the starting configuration is generated by putting an array of copolymer chains onto the lattice in an extended conformation with an end-to-end distance of $(N-1)$ units for each chain. The polymer chains are parallel and along one of the axis. First, a maximum concentration of monomers is reached (in our case the maximum concentration can be 100% or more than 90%). For a given copolymer concentration, the number of polymer chains is less than the maximum value. Randomly chosen chains are taken away from the box until the desired concentration is reached. After the desired number of chains has been taken out, the remaining empty sites were assigned to solvent molecules.

The trial moves consist of two types that are illustrated schematically in Fig. 1.

(i) Exchange movements: A monomer is selected, and it can exchange with a solvent molecule on one of its 18 nearest neighbors. If the exchange does not break the chain, it is allowed [Fig. 1(a)]. If the exchange creates a single break in the chain, the solvent molecule will continue to exchange with subsequent monomers along the chain until reconnection of the links occur [Fig. 1(b)]. If the exchange breaks the chain in two chains, it is not allowed [Fig. 1(c)]. This exchange movement has proved to be very efficient in studying the self-assembly of block copolymers [41,53–55,57].

(ii) Chain reverse: A chain is selected, and all the A monomers on the chain are exchanged with the B monomers on the same chain [Fig. 1(d)]. Our simulation shows that this chain reverse movement further accelerated the equilibrium of the system.

The energy of the system is the objective function in the simulated annealing. There are three effective pair interactions in the system, block A and block B, block A and solvent, and block B and solvent. In this paper we consider the 18 nearest neighbor interactions only. These are modeled by assigning an energy $E_{ij}=\varepsilon_{ij}k_BT_{ref}$ to each nearest neighbor pair of unlike components i and j, where $i, j=A, B$, and S (solvent); ε_{ij} is a reduced interaction energy; k_B is the Boltzmann constant; and T_{ref} is a reference temperature. In our simulations, ε_{AS} is attractive whereas ε_{BS} and ε_{AB} are repulsive, which ensures that the solvent is good to the A segments and poor to the B segments, and the immiscibility between the A and B segments. Furthermore we assume $\varepsilon_{ii}=0$, with $i=A, B, S$.

The usual annealing schedule, $T_j=fT_{j-1}$, was used in the simulations, where T_j is the temperature used in the jth annealing step and f is a scaling factor. The annealing was continued until the temperature reached a predetermined value (T_F). In our studies we used $f=0.9$, $T_1=50T_{ref}$, and the temperature reaches the final $T_F(=T_{80})$ after 80 annealing steps. One Monte Carlo step (MCS) is defined as the time taken for, on average, all the lattice sites to be visited for an attempted move. At each annealing step, 25 000 MCSs are performed. The acceptance or rejection of one attempted move is further governed by the Metropolis rule [58]; namely, it is accepted if the energy change ΔE is negative; otherwise, it is accepted with a probability of p as the following equation: $p=\exp(-\Delta E/k_BT_j)$, where ΔE is the difference in the energy after and before a trial move.

The most important quantity that we calculate is the static collective structure factor $S(\mathbf{q})$. To obtain $S(\mathbf{q})$ from the simulations, we follow Ref. [59] and label the sites with a spin-type variable $\sigma(\mathbf{r}_i)$ which is 1 for B monomers, -1 for A monomers and solvent molecules. The collective structure factor $S(\mathbf{q})$ is then evaluated as

$$S(\mathbf{q}) = L^{-3}\sum_{i,j} e^{i\mathbf{q}\cdot\mathbf{r}_{ij}}\sigma(\mathbf{r}_i)\sigma(\mathbf{r}_j).$$

Here the sum runs over all lattice sites. Given the finite lattices and the boundary conditions implemented here, only a discrete set of q vectors is physically meaningful; these are

$$\mathbf{q} = 2\pi\left(\frac{n_x}{L}, \frac{n_y}{L}, \frac{n_z}{L}\right)$$

with $0\leqslant n_r\leqslant L$ for $r=x,y,z$. We compute the structure factor for all these q vectors and then average over those of equal length to obtain the spherical structure factor $S(|q|)=S(q)$.

RESULTS AND DISCUSSION

A series of diblock copolymers is employed in the study. Specifications of these copolymers, the total chain length (N)

TABLE I. The condition that the gyroid structure forms.

N	N_B	L	ε_{BS}	c_P (%)	c_B (%)
9	7	24	0.5–0.6	52.1–54.1	40.5–42.1
9	7	25	0.4–0.5	52.7–54.1	41.0–42.1
9	6	23	0.9–1.1	59.2–60.4	39.5–40.3
9	6	24	0.6–1.1	58.9–60.4	39.3–40.3
9	6	25	0.9–1.1	58.9–60.2	39.3–40.1
9	5	24	1.4–1.7	71.5–72.2	39.7–40.1
9	5	25	1.5–1.6	71.5–72.2	39.7–40.1
8	5	23	1.4–1.7	61.9–64.0	38.7–40.0
8	5	24	1.4–1.9	63.7–65.0	39.8–40.6
8	5	25	1.0–1.2	64.5–65.3	40.3–40.8

and the B-segment length (N_B), are listed in Table I. Previous studies have indicated that in any simulation methods applied to block copolymer systems, the similation box size must be fine-tuned such that the box is commensurate to the period of the ordered structures [43,46,60]. Due to the cubic symmetry of the gyroid structure, cubic boxes are used in our simulations. The box size is varied to obtain optimum structures. In all the simulations reported here, the A-B and A-S interaction parameters are kept at constant values, $\varepsilon_{AB}=1.0$ and $\varepsilon_{AS}=-1.0$, respectively. The simulations proceed in two steps. The first step of the simulations is to obtain a generic structural transition sequence for the diblock copolymer solutions. Specifically, for a given cubic box, the ground state morphology is obtained for a fixed B-S interaction, $\varepsilon_{BS}=1.0$, and for different copolymer concentrations. For those copolymers listed in Table I in the difference boxes, a series of morphologies, including spherical micellar phase, cylindrical micellar phase, hexagonally packed cylindrical phase, continuous cylindrical phase, perforated lamellar phase, and lamellar phase, are obtained when the copolymer concentration is varied from a low one to a high one. The second step of the simulations is to locate the gyroid phase. Experimentally the gyroid structure is observed in a narrow range of block copolymer concentrations between the hexagonally packed cylindrical and the lamellar phases [34–37]. Therefore we focus our attentions on the copolymer concentrations where the continuous cylindrical or the perforated lamellar phases are observed, while varying the B-S interaction ε_{BS} to locate the gyroid structure. We find that we can always locate the gyroid structure for the copolymers listed in Table I using such a two-step searching procedure. Furthermore, it is observed that the gyroid structure forms at specific box sizes, near $L=24$ with one periodic structure and near $L=48$ with twice periodic structure. Since it is time consuming to carry out simulations for a twice periodic structure, we used the simulation box near $L=24$ for all the simulations reported in this paper.

Figure 2 shows a typical gyroid morphology that formed in our simulation. It is displayed as the isosurface contour plot of the B monomers (only B microphase is shown here for clarity; A and solvent correspond to the empty volume). By direct inspection, we find that this morphology consists of two interpenetrating, but nonintersecting, strut networks

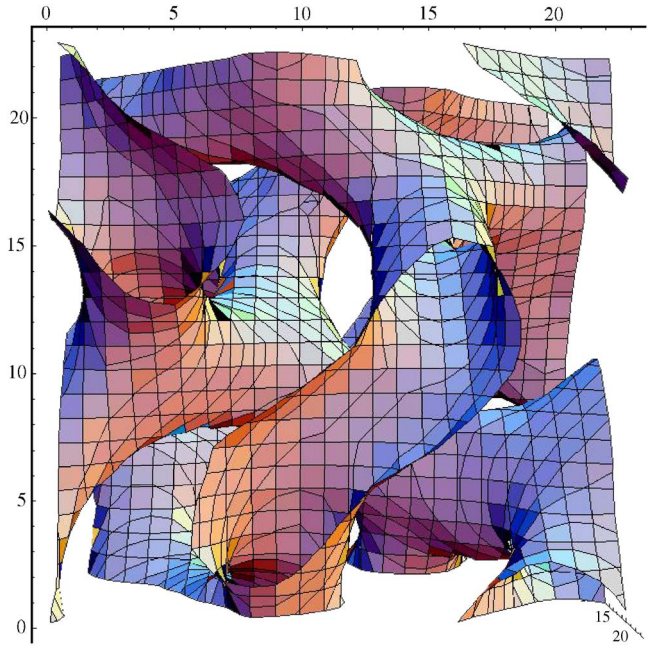

FIG. 2. (Color online) Isosurface contour of the simulated morphology formed by 64.0% $A(3)$-b-$B(5)$ in solvent selective for A segments with $\varepsilon_{BS}=1.5$ on a $24\times24\times24$ lattice.

of the B monomers, corresponding to the characteristic of the gyroid morphology reported experimentally. [9–14]. Previous simulation papers on amphiphilic or block copolymer systems using Monte Carlo method or using free-energy-based Langevin diffusion equations have reported the reproduction of structures resembling the gyroid [42–48].

The simulations demonstrate that the formation of the gyroid structure is restricted to a narrow range of copolymer concentrations. Furthermore, gyroid formation is especially sensitive to the B-S interaction ε_{BS}. Table I lists the parameters that form the gyroid structure. For a given box size, one typical simulated phase diagram of the studied system is shown in Fig. 3. It is clear from the phase diagram that the hexagonally packed cylindrical phase, the perforated lamellar phase (PL), the gyroid phase, and the lamellar phase can

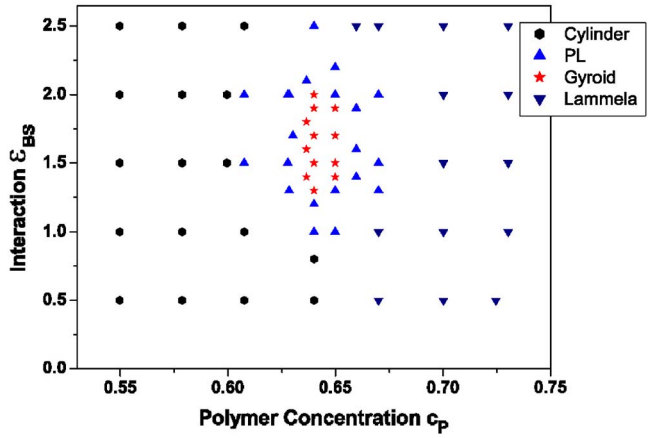

FIG. 3. (Color online) The simulated phase diagram of $A(3)$-b-$B(5)$ in solvent selective for A segment on a $24\times24\times24$ lattice.

be observed when the copolymer concentration is increased. The gyroid structure is in a narrow range of block copolymer concentrations between the hexagonally packed cylindrical and the lamellar phases, and the PL structure is found between the hexagonally packed cylindrical and the gyroid and between the gyroid and lamellar phases. The PL structure has also been observed during the $L \leftrightarrow G$ transition in diblock copolymer melts [17] and during the $G \leftrightarrow C$ transition in diblock copolymer solutions [38,39]. It has been identified as a long-lived nonequilibrium state [10,61–64]. For all the copolymers with compositions and box size listed in Table I, the simulated phase diagram is very similar to that shown in Fig. 3, except that gyroid region in the phase diagram is displaced. For a given block copolymer composition, the regions of the hexagonally packed cylindrical phase, the sum of the perforated lamellar phase and the gyroid phase, and the lamellar phase do not change with the box size, whereas the region of the gyroid phase does. Table I has listed the gyroid region. When tested with other box sizes not listed in Table I, the hexagonally packed cylindrical and the lamellar phase regions in the phase diagram did not change, whereas the gyroid region in the phase diagram is replaced by the PL phase.

Table I illustrated that for a copolymer with a given chain length and composition, the gyroid structure can be formed in a narrow range of box size. This case was also found in Monte Carlo simulations of symmetric diblock copolymers in solution [43] and of blends of triblock copolymer and homopolymer [46]. The box length that the gyroid structure can be observed concentrates on $L=23-25$ for these studied chain lengths and compositions, which reflect that the period of the simulated gyroid phase lies in this length scale. It is interesting to notice that, in the region where the gyroid is stable, the *B*-monomers, which form the strut networks of the gyroid structure, are kept at an almost constant concentration ($c_B \sim 40\%$). To keep this constant *B*-monomer concentration, the total polymer concentration (c_P) must increase with the decrease of the *B*-segment length for copolymers with a given chain length (N). Table I also shows that, in the gyroid phase region, the *B*-*S* interaction (ε_{BS}) increases with the decrease of N_B, that is, for a fixed chain length and smaller N_B, the gyroid structure will form in solvents with stronger selectivity than for those with longer N_B.

The predicted conditions for the formation of the gyroid structures can be compared with experiments. Using variable-temperature small-angle x-ray scattering (SAXS), Lai *et al.* [36] studied the phase behavior of poly(styrene-*b*-isoprene) (S-*b*-I) diblock copolymers in the isoprene-selective solvents tetradecane (TD), tributylamine (TBA), and squalane (SQ), with the selectivity going in the order of SQ > TD > TBA. Their results show that the gyroid structures are stable over limited regions near an order-disorder transition locus. The composite (S-*b*-I)-TD phase map for 88 samples (10 melts and 78 solutions) in their experiments shows that the gyroid structure (G_S) forms at almost constant weight fraction of polystyrene in the solution (about 35–40 %). Their experiments also show that whether the gyroid structure (G_S) can be formed in solutions also depends on the solvent selectivity. For samples with relatively higher polystyrene content [S(24)-*b*-I(6)], the gyroid structure (G_S) can be observed in solvent (TD) with relatively lower selectivity, but not in solvents (SQ) with higher selectivity; whereas for samples with relatively lower polystyrene content [S(19)-*b*-I(7)], the gyroid structure (G_S) can be observed in solvents (SQ and TD) with relatively higher selectivity, but not in solvents (TBA) with lower selectivity. The polystyrene in those experiments corresponds to the *B* segment in our models, thus it can be concluded that our simulation results have the same trends with these experimental facts.

Using SAXS, rheology, and static birefringence, Lodge and co-workers [34,35,37] studied the phase behavior of six poly(styrene-*b*-isoprene) (S-*b*-I) diblock copolymers with different composition, in the styrene-selective solvents di-*n*-butyl phthalate (DBP), diethyl phthalate (DEP), and dimethyl phthalate (DMP), with the selectivity going in the order of DMP > DEP > DBP. Phase diagrams for their samples also show that for sample with relatively higher polyisoprene content [S(11)-*b*-I(32)], the gyroid structure (G_I) can be observed in solvents (DBP) with relatively lower selectivity, but not in solvents (DEP) with higher selectivity. The phase diagrams for their samples also show that the polymer concentrations where the gyroid structure (G_I) forms increase with the decrease of polyisoprene content. The polyisoprene in those experiments corresponds to the *B* segment in our models. Thus the above analysis shows that all these experimental facts are consistent with our simulation results.

Transmission electron micrograph (TEM) images of the gyroid structure when viewed along the [lll] axis of the $Ia\bar{3}d$ unit cell have the "wagon wheel" pattern shown in Fig. 4(a). This image was obtained by Lammertink *et al.* [9] on the blends of the diblocks poly(styrene-block-ferrocenyldimethylsilane) copolymers 9/19 with homopolymer. By generating such a projection along the [111] axis for the simulated gyroid structure, one obtains the image shown in Fig. 4(b), which is very similar to the experimental image in Fig. 4(a). A similar pattern was also obtained in Monte Carlo simulations of symmetric diblock copolymers in solution [43].

Projections such as Fig. 4 do not allow the gyroid structure to be clearly distinguished from the "double diamond" phase, which is a cubic phase closely related to the gyroid. SAXS techniques have been instrumental in the determination of the gyroid structures [34–38]. SAXS spectra give peak patterns that can be used as fingerprints in determining structures. The calculated spherically averaged structure factor of the simulated structure of Fig. 2 is shown in Fig. 5, where the experimental SAXS peaks of the gyroid structure [34] are indicated by the arrows. The spherically averaged structure factor of the simulated structure is in good agreement with the experimental SAXS spectra [34] of the gyroid structure. Therefore one can incontestably identify the simulated structure as that of the gyroid. For gyroid structures formed under the conditions listed in Table I, all have the very similar snapshots as that shown in Fig. 2, and all have the very similar spherically averaged structure factor as that shown in Fig. 5. Especially, all structures have very good reproducibility.

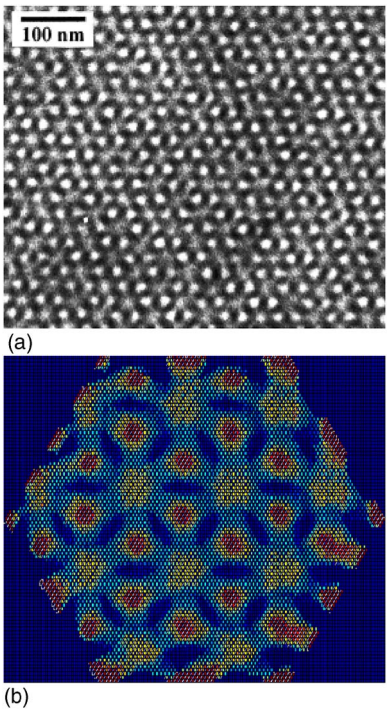

FIG. 4. (Color online) (a) Bright-field TEM micrograph of blends of the diblocks poly(styrene-block-ferrocenyldimethylsilane) copolymers 9/19 with homopolymer displaying the [111] projection (wagon wheel) of the gyroid morphology [9]. (b) Wagon wheel image of gyroid structure formed for the system in Fig. 2. The image was formed by projection along the 111 axis, which was periodically extended to two periods in three directions.

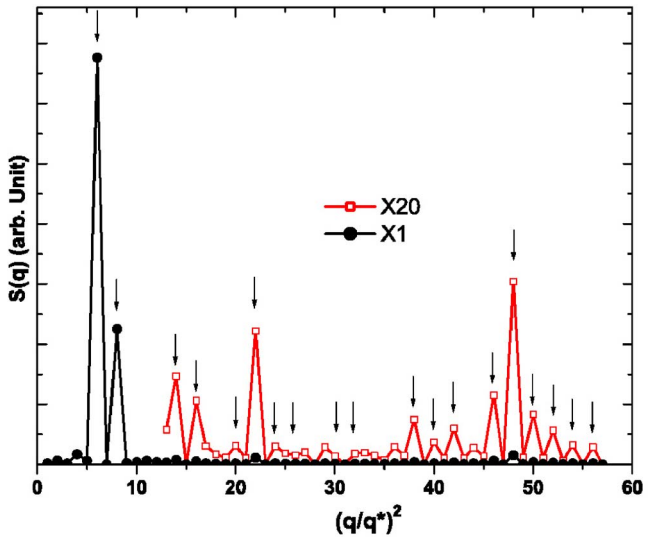

FIG. 5. (Color online) The calculated spherically averaged structure factor of the simulated gyroid structure formed for the system in Fig. 2; the calculated data (●) and the magnified version (○) are indicated in the figure; the arrows indicate reflections corresponding to the allowed q/q^* ratios for the G structure of $\sqrt{6}$; $\sqrt{8}$; $\sqrt{14}$; $\sqrt{16}$; $\sqrt{20}$; $\sqrt{22}$; $\sqrt{24}$; $\sqrt{26}$; $\sqrt{30}$; $\sqrt{32}$; $\sqrt{38}$; $\sqrt{40}$; $\sqrt{42}$; $\sqrt{46}$; $\sqrt{48}$; $\sqrt{50}$;$\sqrt{52}$; $\sqrt{54}$;$\sqrt{56}$ [34], where $\mathbf{q}^*=2\pi/L$.

CONCLUSIONS

The simulated annealing method was applied to study the condition of the formation of the gyroid structure in diblock copolymer solutions composed of $A(N_A)$-b-$B(N_B)$ diblock copolymers (with $N_A<N_B$) in A-selective solvents. A series of copolymer compositions is studied. Phase diagrams of the system are constructed. The predicted conditions for the formation of gyroids are in good agreement with available experiments. Very regular gyroid morphologies are reproduced. The study demonstrated that the simulated annealing method is an efficient tool for the study of the formation of complex structures from block copolymers. We hope that the simulated gyroid structure can be used as a good input for the study of OOTs involving the gyroid in diblock copolymer solutions.

ACKNOWLEDGMENTS

This research was financially supported by the National Natural Science Foundation of China (Grant Nos. 20474034, 20374031, 20373029), and by the Chinese Ministry of Education with the Joint-Research Foundation of the Nankai and Tianjin Universities, and the Foundation for University Key Teacher (Grant No. GG-703-10055-1008), and by Nankai University ISC. A.C.S. acknowledges the support by the Natural Science and Engineering Council (NSERC) of Canada.

[1] M. W. Matsen and M. Schick, Phys. Rev. Lett. **72**, 2660 (1994).
[2] Z. Tuzar and P. Kratochvil, in *Surface and Colloid Science*, edited by E. Matijevic (Plenum Press, New York, 1993), Vol. 15.
[3] F. S. Bates and G. H. Fredrickson, Annu. Rev. Phys. Chem. **41**, 525 (1990).
[4] G. H. Fredrickson and F. S. Bates, Annu. Rev. Mater. Sci. **26**, 501 (1996).
[5] I. W. Hamley, *The Physics of Block Copolymer* (Oxford University Press, New York, 1998).
[6] N. Hadjichristidis, S. Pispas, and G. Floudas, *Block Copolymers: Synthetic Strategies, Physical Properties, and Applications* (John Wiley & Sons, New York, 2002).
[7] M. W. Matsen and F. S. Bates, Macromolecules **29**, 7641 (1996); **29**, 1091 (1996).
[8] S. T. Molner and P. D. Olmsted, J. Phys. II **7**, 249 (1997).
[9] R. G. H. Lammertink, M. A. Hempenius, E. Thomas, and G. J. Vancso, J. Polym. Sci., Part B: Polym. Phys. **37**, 1009 (1999).
[10] S. Forster, A. K. Khandpur, J. Zhao, F. S. Bates, I. W. Hamley, A. J. Ryan, and W. Bras, Macromolecules **27**, 6922 (1994).
[11] D. A. Hajduk, P. E. Harper, S. M. Gruner, C. C. Honeker, G. Kim, E. L. Thomas, and L. J. Fetters, Macromolecules **27**, 4063 (1994).

[12] D. A. Hajduk, P. E. Harper, S. M. Gruner, C. C. Honeker, E. L. Thomas, and L. J. Fetters, Macromolecules **28**, 2570 (1995).
[13] R. J. Spontak, J. C. Fung, M. B. Braunfeld, J. W. Sedat, D. A. Agard, L. Kane, S. D. Smith, M. M. Satkowski, A. Ashraf, D. A. Hajduk, and S. M. Gruner, Macromolecules **29**, 4494 (1996).
[14] J. H. Laurer, D. A. Hajduk, J. C. Fung, J. W. Sedat, S. D. Smith, S. M. Gruner, D. A. Agard, and R. J. Spontak, Macromolecules **30**, 3938 (1997).
[15] M. W. Matsen, J. Phys.: Condens. Matter **14**, R21 (2002).
[16] D. A. Hajduk, H. Takenouchi, M. A. Hillmyer, F. S. Bates, M. E. Vigild, and K. Almdal, Macromolecules **30**, 3788 (1997).
[17] D. A. Hajduk, R. M. Ho, M. A. Hillmyer, F. S. Bates, and K. Almdal, J. Phys. Chem. B **102**, 1356 (1998).
[18] S. Sakurai, H. Umeda, C. Furukawa, H. Irie, S. Nomura, H. H. Lee, and J. K. Kim, J. Chem. Phys. **108**, 4333 (1998).
[19] I. W. Hamley, J. P. A. Fairclough, A. J. Ryan, S.-M. Mai, and C. Booth, Phys. Chem. Chem. Phys. **1**, 2097 (1999).
[20] M. F. Schulz, F. S. Bates, K. Almdal, and K. Mortensen, Phys. Rev. Lett. **73**, 86 (1994).
[21] M. E. Vigild, K. Almdal, K. Mortensen, I. W. Hamley, J. P. A. Fairclough, and A. J. Ryan, Macromolecules **31**, 5702 (1998).
[22] G. Floudas, R. Ulrich, and U. Wiesner, J. Chem. Phys. **110**, 652 (1999).
[23] M. Laradji, A.-C. Shi, J. Noolandi, and R. C. Desai, Macromolecules **30**, 3242 (1997).
[24] M. W. Matsen, Phys. Rev. Lett. **80**, 4470 (1998).
[25] K. Yamada, M. Nonomura, and T. Ohta, Macromolecules **37**, 5762 (2004).
[26] S. Jain and F. S. Bates, Science **300**, 460 (2003).
[27] S. Forster, B. Berton, H.-P. Hentze, E. Kramer, M. Antonietti, and P. Lindner, Macromolecules **34**, 4610 (2001).
[28] Y.-Y. Won, H. T. Davis, and F. S. Bates, Science **283**, 960 (1999).
[29] L. Zhang, R. J. Barlow, and A. Eisenberg, Macromolecules **28**, 6055 (1995).
[30] G. Riess, Prog. Polym. Sci. **28**, 1107 (2003).
[31] K. Mortensen, Curr. Opin. Colloid Interface Sci. **3**, 12 (1998).
[32] P. Alexandridis and R. J. Spontak, Curr. Opin. Colloid Interface Sci. **4**, 130 (1999).
[33] M. Svensson, P. Alexandridis, and P. Linse, Macromolecules **32**, 637 (1999).
[34] K. J. Hanley and T. P. Lodge, J. Polym. Sci., Part B: Polym. Phys. **36**, 3101 (1998).
[35] K. J. Hanley, T. P. Lodge, and C.-I. Huang, Macromolecules **33**, 5918 (2000).
[36] C. Lai, W. B. Russel, and R. A. Register, Macromolecules **35**, 841 (2002).
[37] T. P. Lodge, B. Pudil, and K. J. Hanley, Macromolecules **35**, 4707 (2002).
[38] C. Y. Wang and T. P. Lodge, Macromolecules **35**, 6997 (2002).
[39] C. Y. Wang and T. P. Lodge, Macromol. Rapid Commun. **23**, 49 (2002).
[40] I. W. Hamley, V. Castelletto, O. O. Mykhaylyk, Z. Yang, R. P. May, K. S. Lyakhova, G. J. A. Sevink, and A. V. Zvelindovsky, Langmuir **20**, 10785 (2004).
[41] B. Yu, B. Li, P. Sun, T. Chen, Q. Jin, D. Ding, and A.-C. Shi, J. Chem. Phys. **123**, 234902 (2005).
[42] W. T. Gozdz and R. Hołyst, Macromol. Theory Simul. **5**, 321 (1996).
[43] R. G. Larson, J. Phys. II **6**, 1441 (1996).
[44] R. D. Groot and T. J. Madden, J. Chem. Phys. **108**, 8713 (1998); R. D. Groot, T. J. Madden, and D. J. Tildesley, *ibid.* **110**, 9739 (1999).
[45] M. Nonomura and T. Ohta, J. Phys.: Condens. Matter **13**, 9089 (2001); , Physica A **304A**, 77 (2002); M. Imai, A. Saeki, T. Teramoto, A. Kawaguchi, K. Nakaya, T. Kato, and K. Ito, J. Chem. Phys. **115**, 10525 (2001).
[46] T. Dotera, Phys. Rev. Lett. **89**, 205502 (2002).
[47] M. Nonomura, K. Yamada, and T. Ohta, J. Phys.: Condens. Matter **15**, L423 (2003).
[48] N. González-Segredo and P. V. Coveney, Phys. Rev. E **69**, 061501 (2004).
[49] S. Kirkpatrick, C. D. Gelatt, and M. P. Vecchi, Jr., Science **220**, 671 (1983); S. Kirkpatrick, J. Stat. Phys. **34**, 975 (1984).
[50] G. S. Grest, C. M. Soukoulis, and K. Levin, Phys. Rev. Lett. **56**, 1148 (1986); A. Chakrabarti and R. Toral, Phys. Rev. B **39**, 542 (1989).
[51] R. G. Larson, J. Chem. Phys. **96**, 7904 (1992); **91**, 2479 (1989).
[52] A. Chakrabarti and J. D. Gunton, Phys. Rev. E **47**, R792 (1993).
[53] P. Sun, Y. Yin, B. Li, Q. Jin, and D. Ding, Int. J. Mod. Phys. B **17**, 241 (2003).
[54] P. Sun, Y. Yin, B. Li, T. Chen, Q. Jin, D. Ding, and A.-C. Shi, J. Chem. Phys. **122**, 204905 (2005).
[55] Y. Yin, P. Sun, T. Chen, B. Li, Q. Jin, D. Ding, and A.-C. Shi, ChemPhysChem **5**, 540 (2004).
[56] I. Carmesin and K. Kremer, Macromolecules **21**, 2819 (1988).
[57] J. Ding, T. J. Carver, and A. H. Windle, Comput. Theor. Polym. Sci. **11**, 483 (2001).
[58] N. Metropolis, A. W. Rosenbluth, M. N. Rosenbluth, A. H. Teller, and E. Teller, J. Chem. Phys. **21**, 1087 (1953).
[59] H. Fried and K. Binder, J. Chem. Phys. **94**, 8349 (1991).
[60] U. Micka and K. Binder, Macromol. Theory Simul. **4**, 419 (1995); Y. Bohbot-Raviv and Z.-G. Wang, Phys. Rev. Lett. **85**, 3428 (2000).
[61] A. K. Khandpur, S. Forster, F. S. Bates, I. W. Hamley, A. J. Ryan, W. Bras, K. Almdal, and K. Mortensen, Macromolecules **28**, 8796 (1995).
[62] J. Zhao, B. Majumdar, M. F. Schulz, F. S. Bates, K. Almdal, K. Mortensen, D. A. Hajduk, and S. M. Gruner, Macromolecules **29**, 1204 (1996).
[63] M. F. Schulz, A. K. Khandpur, F. S. Bates, K. Almdal, K. Mortensen, D. A. Hajduk, and S. M. Gruner, Macromolecules **29**, 2857 (1996).
[64] K. Almdal, K. Mortensen, A. J. Ryan, and F. S. Bates, Macromolecules **29**, 5940 (1996).